RAYTHEON COMPANY
EQUIPMENT DIVISION

RAYTHEON

12
8

FINAL REPORT

LASER DOPPLER RADAR FOR REMOTE ATMOSPHERIC SOUNDING

LEVEL II

Contract N00014-75-C-0282

ER79-4105

January 1979

Prepared by

RAYTHEON COMPANY
EQUIPMENT DEVELOPMENT LABORATORIES
ADVANCED DEVELOPMENT LABORATORY
ELECTRO-OPTICS DEPARTMENT
WAYLAND, MASSACHUSETTS 01778

For

OFFICE OF NAVAL RESEARCH
DEPARTMENT OF THE NAVY
800 N. QUINCY ST.
ARLINGTON, VIRGINIA 22217

This research was sponsored by the Office of Naval Research.
(Authority-NR377-020/3-11-76(421)

UNCLASSIFIED

SECURITY CLASSIFICATION OF THIS PAGE (When Data Entered)

REPORT DOCUMENTATION PAGE	READ INSTRUCTIONS BEFORE COMPLETING FORM
1. REPORT NUMBER	2. GOVT ACCESSION NO. (9) 3. RECIPIENT'S CATALOG NUMBER
4. TITLE (and Subtitle) (6) Laser Doppler Radar for Remote Atmospheric Sounding.	5. TYPE OF REPORT & PERIOD COVERED Final Report. 8 Jan 75 - 8 Jan 78
	6. PERFORMING ORG. REPORT NUMBER (14) ER79-4105
7. AUTHOR(s) (10) Charles A./DiMarzio, Douglas W./Toomey, Albert V./Jelalian	8. CONTRACT OR GRANT NUMBER(s) (15) N0014-75-C-0282
9. PERFORMING ORGANIZATION NAME AND ADDRESS Raytheon Company, Equipment Division, Electro-Optics Dept, Wayland, Massachusetts 01778	10. PROGRAM ELEMENT, PROJECT, TASK AREA & WORK UNIT NUMBERS NR377-020/3-11-76(421)
11. CONTROLLING OFFICE NAME AND ADDRESS (11) Office of Naval Research, 800 N. Quincy St., Code 421, Arlington, Virginia 22217	12. REPORT DATE January 1979
	13. NUMBER OF PAGES 36
14. MONITORING AGENCY NAME & ADDRESS(if different from Controlling Office) Same as Controlling Office (12) 40p.	15. SECURITY CLASS. (of this report) Unclassified
	15a. DECLASSIFICATION/DOWNGRADING SCHEDULE

16. DISTRIBUTION STATEMENT (of this Report)
Reproduction in whole or in part is permitted for any purpose of the U.S. Government, approved for Public Release, distribution unlimited

17. DISTRIBUTION STATEMENT (of the abstract entered in Block 20, if different from Report)

18. SUPPLEMENTARY NOTES

19. KEY WORDS (Continue on reverse side if necessary and identify by block number)
Laser, Laser Doppler, Turbulence, Turbulence Spectrum, CO_2 Laser System, Atmospheric, Atmospheric Kinetic Energy, Radar, Doppler Radar, Coherent Detection, Weather Prediction, LIDAR

20. ABSTRACT (Continue on reverse side if necessary and identify by block number)
Measurements have been made of the atmospheric velocity turbulence spectrum using a mobile, CO_2, continuous wave, Doppler LIDAR system. The LIDAR was used in a heterodyne configuration with a 30 cm output optics to produce a conical scan. Velocity data from this scan were Fourier analyzed to obtain the velocity power density spectrum. The -5/3 power law of Kolmogorov was observed along with variations in total energy which could be

→ next page

DD FORM 1 JAN 73 1473 EDITION OF 1 NOV 65 IS OBSOLETE

UNCLASSIFIED

SB

SECURITY CLASSIFICATION OF THIS PAGE (When Data Entered)

388 201

Block 20. ABSTRACT (Continued)

correlated with storm activity. In addition, departures from the Kolmogorov spectrum were observed under some conditions. It is hoped that the total energy and departure from the -5/3 power law may prove useful in short-term meteorological forecasting.

TABLE OF CONTENTS

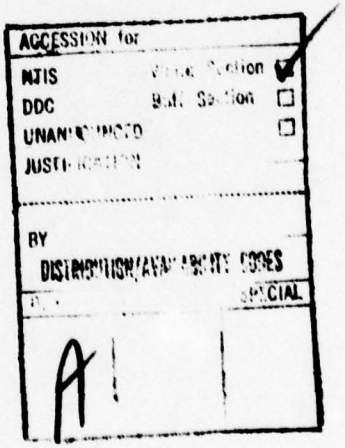

LIST OF ILLUSTRATIONS

1. INTRODUCTION

Throughout modern time, man has strived for accurate weather prediction, with a need for ever increasing amounts of wind velocity data. In the early days of meteorology, wind velocities were measured at widely separated points to determine the large-scale features of the wind velocity field. This provided only a coarse picture of a phenomenon known to have small scale features of interest. With the advent of the electronic computer, it became feasible to process the large amounts of data that newly developed laser systems could now deliver. Thus the analysis of minute details of wind behavior became practical.

A coherent detection, CO_2, continuous wave Laser Doppler Velocimeter (LDV) is a useful instrument for these remote wind velocity measurements. The present paper describes the use of a LDV to determine the power spectral density of a turbulent wind velocity field, and thus illustrates the power of the LDV for collecting, analyzing, and displaying large amounts of wind velocity data.

The success of the system is due to a combination of the small scale remote measurement capability of the laser with the numerical analysis capability of a computer, which can reduce large quantities of data to meaningful displays. A sample of several hundred thousand wind velocity measurements is reduced to an energy spectral density curve with easily recognizable

features. This system has been used to verify the -5/3 power law of Kolmogorov at spatial frequencies from 1/30 to 1/2 km^{-1}.

This system is the result of more than ten years of research and development of CO_2 laser systems. The first measurement of the Doppler shift in CO_2 radiation backscattered from the atmosphere was made in 1964. By 1974, sophisticated systems, using computers for real time processing, had been used for measuring the behavior of aircraft wakes and dust devils. Atmospheric measurements have been made at ranges up to 1 km with CW, 20 watt systems and 8 kn with 25 mJ pulsed systems.

The coherent CO_2 LDV is ideally suited for measurement of the line-of-sight velocity component as a function of range and time. Measurement of a three dimensional velocity vector requires at least three independent measurements. These may be made directly by focussing three systems into the same volume of space from different angles, or may be inferred either from successive measurements at a given point in space with a moving system, or from closely timed measurements at slightly different points in space using a fixed system. The moving system approach assumes that the velocity vector does not change in the measurement time, while the fixed system approach assumes that the velocity vector does not vary over the space required for the measurement. The present system uses the fixed system

approach by generating a conical scan about a vertical axis. A 30° cone half angle is used so the diameter of the circle described in space is equal to the slant range to the focus of the transmitted beam. The velocity vector at the center of the circle is inferred from the measurements of the line-of-sight velocity around its circumference.

This paper begins with a brief description of the assumed wind velocity field and the required measurements and calculations. The principles of obtaining velocity measurements with an LDV using a conical scan, and the principles of using this velocity to obtain the turbulent velocity energy spectral density are described. Then the system is described in detail, followed by the processing methods, results, and conclusions. It will be shown that the LDV provides a useful tool for measurement of mesoscale atmospheric behavior with a capability for obtaining, processing, and analyzing large quantities of data concerning wind velocity fields.

2. THE TURBULENT KINETIC ENERGY DENSITY SPECTRUM

The wind velocity is a complicated function which varies randomly with position and time. Thus, even if the wind velocity is accurately measured at a large number of points, the results may not be easily interpreted. Some method of simplifying the data to present meaningful results in usable form is required. One approach to this problem is Fourier analysis. The behavior of the wind velocity at a given time may be

expressed by the vector velocity $\bar{V}(\bar{r})$ as a function of position, or, equivalently by its spectrum $\tilde{\bar{V}}(\bar{k})$ where k is defined as a spatial frequency. These variables are a Fourier transform pair:

$$\bar{V}(\bar{r}) = \frac{1}{(2\pi)^{3/2}} \iiint \tilde{\bar{V}}(\bar{k})\, e^{i\bar{k}\cdot\bar{r}}\, d^3k$$

$$\tilde{\bar{V}}(\bar{k}) = \frac{1}{(2\pi)^{3/2}} \iiint \bar{V}(\bar{r})\, e^{i\bar{k}\cdot\bar{r}}\, d^3r$$

While these two representations contain identical information, it is reasonable to expect that one or the other may present the information in a way which is more understandable and more directly related to the physics of the problem. For the present purpose, it is the velocity spectrum which proves to be most useful. Representation of the wind velocity in terms of its spectrum is equivalent to stating that the velocity field consists of many sinusoidal waves having different amplitudes and phases. The square of the amplitude $|\tilde{\bar{V}}(\bar{k})|^2$ has units of $\left[\text{energy mass}^{-1} \quad (\text{spatial frequency})^{-3}\right]$, and represents the amount of Kinetic energy per unit mass of atmosphere per unit volume of frequency space.

It should be evident that this would be useful in studying the distribution of Kinetic energy in the atmosphere. Theoretical treatment of the problem by Kolmogorov[1,2,3] has indicated a -5/3 power law should exist for this function;

$$E \equiv |\tilde{\bar{V}}(\bar{k})|^2 = A\epsilon^{2/3}k^{-5/3}$$

where A is a constant of magnitude near ½ and ϵ is the rate of dissipation of turbulent energy per unit mass. Kinetic energy normally enters the atmosphere at low spatial frequencies (large wavelengths), as a result of interaction of the atmosphere with large features of the landscape, pressure gradients and other large-scale causes. Kinetic energy is removed by conversion to thermal energy most easily at small wavelengths. While these processes occur, the atmosphere redistributes energy throughout the spectrum in an attempt to maintain the -5/3 power law. When a change in the energy balance occurs, the -5/3 power law should be temporarily upset at certain wavelengths until the equilibrium is reestablished. Thus, one could speculate that measurement of the energy spectral density should yield information on impending weather changes, by indicating change in the energy balance of the atmosphere. In particular, an increase in the energy at long wavelengths, above that anticipated by the -5/3 law, could indicate that the total energy in the atmosphere is increasing. Such an increase would most likely be followed by a storm in which the energy could redistribute itself according to the -5/3 power law. Thus, the energy spectrum of turbulent wind velocity is an important variable in meteorological research.

It is often convenient to use the autocorrelation function of a random variable as a way of characterizing the size scale

over which the variable changes. This function is the Fourier transform of the energy density spectrum and may readily be obtained from experimental data. The autocorrelation function is given by

$$\Gamma(\Delta\bar{r}) = \langle V(\bar{r})\ V(\bar{r}-\Delta\bar{r})\rangle$$

where the brackets denote an ensemble average. If the atmosphere is homogeneous, the ensemble average may be replaced by a spatial average over a sample of space. This provides a simple way of obtaining the correlation function and thus the energy spectrum. The correlation function in one dimension is obtained by averaging over x as

$$\Gamma(\Delta x) = \frac{1}{(x_2-x_1)} \int_{x_1}^{x_2} \bar{V}(x) \cdot \bar{V}(x - \Delta x)\ dx$$

The energy spectrum is then simply the Fourier transform of the function.

Finally, it has been postulated that it is possible to measure $\Gamma(\Delta x)$ at a single point in space by making a measurement over a period of time and invoking Taylor's Hypothesis.[4] This hypothesis states that the temporal and spatial correlation functions are equivalent if the time is multiplied by the mean wind velocity;

$$\langle V(x,t)V(x,\ t+\tau)\rangle = \langle V(x,t)V(x-\bar{u}\tau\ ,t)\rangle$$

This is often referred to as the assumption of frozen turbulence. That is, the turbulent wind field as viewed by an observer moving at the mean wind velocity changes more slowly than that measured by a stationary observer. The gusts, viewed from a stationary position, are thus slowly changing eddies being transported by the mean wind. This assumption allows a particularly simple measurement of $|\bar{V}|$ as a function of time, at one location, to be used to construct the correlation function, $\Gamma(x)$. Furthermore, for isotropic turbulence, this leads directly to the three dimensional correlation function $\Gamma(\bar{r})$, and thus to the energy density spectrum $E(\bar{k})$.

3. PRINCIPLES OF OPERATION OF THE SYSTEM

The principles of operation of the Coherent CO_2 LDV include three areas of interest: the first is the use of the Doppler shift to obtain a line-of-sight velocity measurement, the second is interpretation of a series of different line-of-sight velocity measurements to obtain a three dimensional velocity vector, and the third is the use of a series of vector velocities obtained at different times to infer the turbulent velocity power density spectrum. In this section, each of these will be discussed in turn.

The measurement of a single component of velocity by the coherent CO_2 LDV may be understood with the aid of Figure 1. A laser beam is transmitted through an interferometer, which passes most of the energy to the target, and diverts a small amount to the detector as shown in Figure 1a. The transmitted

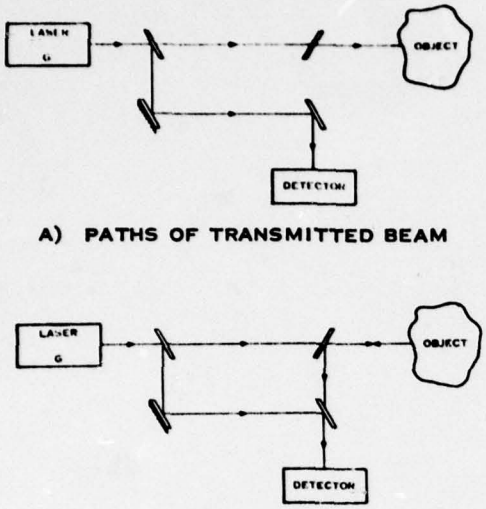

EOA-106

Fig. 1. Doppler LIDAR Transmission and Reception.

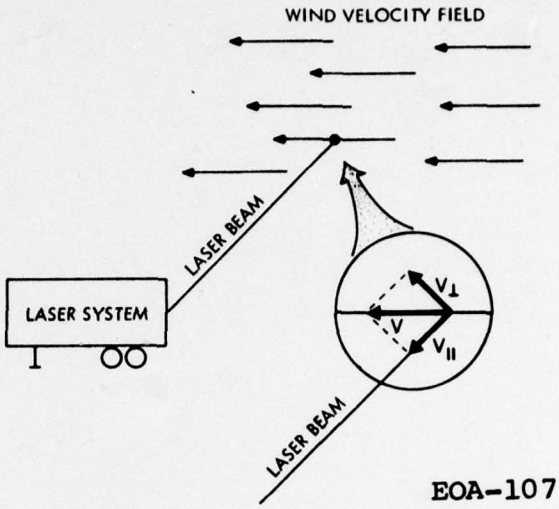

EOA-107

Fig. 2. Velocity Component Sensed by the LIDAR.

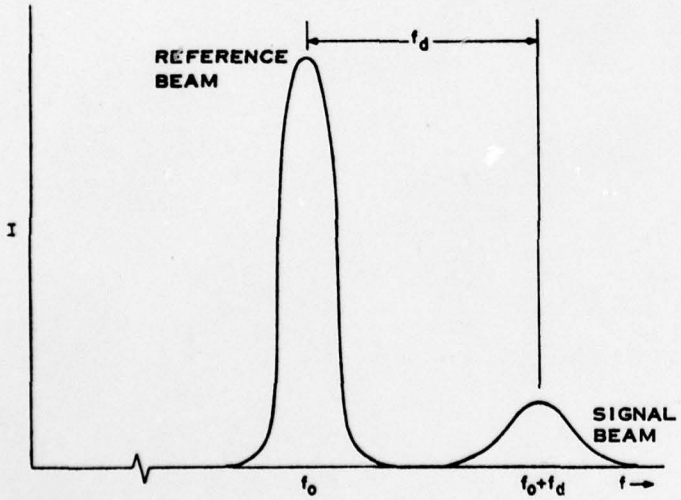

EOA-108

Fig. 3. Spectral Distribution of Power on the Detector.

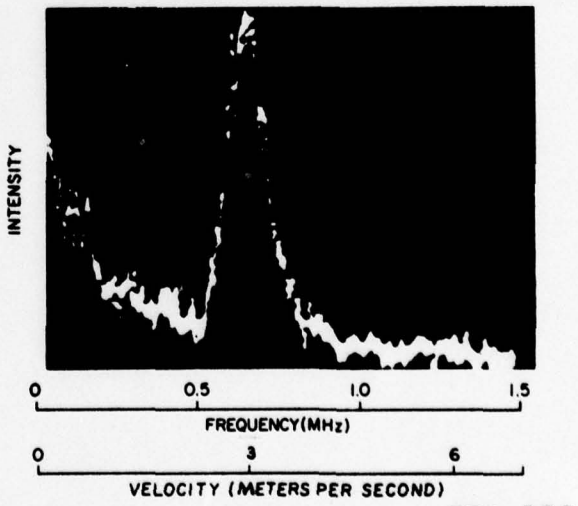

EOA-109

Fig. 4. Typical Lidar Doppler Signal Spectrum.

beam is usually passed through a telescope to the target, which, in the present case, consists of naturally suspended aerosols in the atmosphere. Some of the transmitted energy is back-scattered by the target particles, and enters the detector by the path shown in Figure 1b. According to the Doppler principle this returning energy has been shifted in frequency as illustrated in Figure 3. When these beams are superimposed, the result contains a contribution at the difference frequency, f_d.

The difference frequency is the Doppler frequency, which is proportional to the magnitude of the target velocity component, $V_{||}$. A sample spectrum in Figure 4 shows the intensity as a function of frequency for an actual LDV atmospheric return. It may be seen that there is a peak at .7 MHz corresponding to a velocity of about 3.3 meters per second. It will be noticed that the sign of the velocity has been lost at this point.

The upward looking VAD (velocity-azimuth display) scan is useful for measuring three components of the wind velocity at a point above the system. The scan configuration is as shown in Figure 5. The focussed laser beam is made to scan a cone about a vertical axis with the focus at a range, R, giving the desired altitude, h. In a uniform wind field, the velocity along the line-of-sight for a vertical-axis conical scan is:

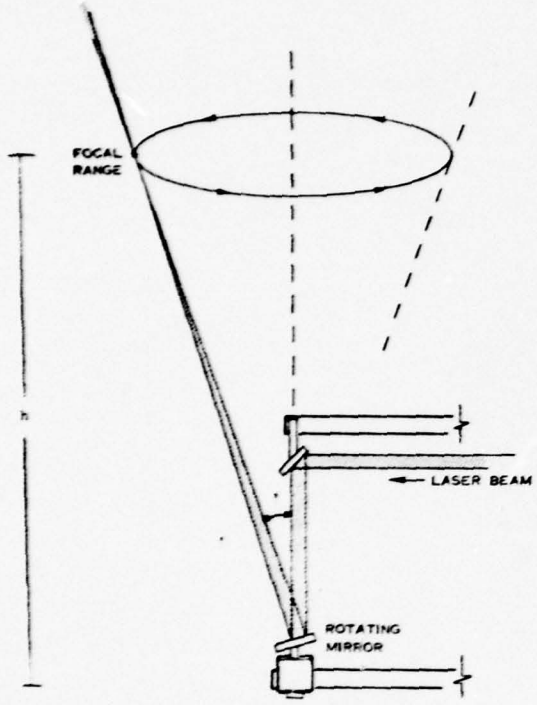

Fig. 5. Upward Looking VAD Scan Concept. EOA-332

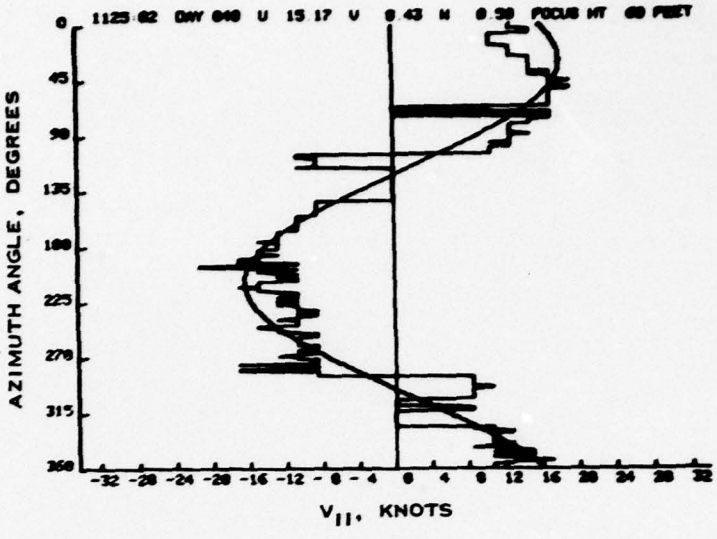

EOA-333

Fig. 6. Typical VAD Scan Data.

1136:11	DAY 094	U	9.56	V	8.03	W	2.92
1136:18	DAY 094	U	10.53	V	8.05	W	1.61
1136:25	DAY 094	U	11.00	V	-5.78	W	-0.85
1136:32	DAY 094	U	10.04	V	9.37	W	1.68
1136:40	DAY 094	U	10.02	V	9.03	W	1.74
1136:49	DAY 094	U	9.81	V	9.30	W	1.83
1136:57	DAY 094	U	4.09	V	11.04	W	0.61
1137:04	DAY 094	U	7.63	V	10.49	W	1.46
1137:11	DAY 094	U	6.08	V	11.61	W	1.09
1137:18	DAY 094	U	10.89	V	8.43	W	1.72
1137:25	DAY 094	U	0.29	V	-12.23	W	-0.40
1137:33	DAY 094	U	10.68	V	8.58	W	1.70
1137:40	DAY 094	U	12.72	V	-10.36	W	-0.62
1137:47	DAY 094	U	9.26	V	10.02	W	1.74
1137:54	DAY 094	U	10.68	V	- 9.05	W	-0.10
1138:02	DAY 094	U	13.78	V	5.72	W	-0.74
1138:09	DAY 094	U	10.96	V	-12.88	W	1.26
1138:16	DAY 094	U	2.35	V	12.02	W	1.34
1138:23	DAY 094	U	12.44	V	5.06	W	-0.01
1138:30	DAY 094	U	9.90	V	- 8.81	W	0.19
1138:38	DAY 094	U	7.54	V	- 7.25	W	-0.43

(VELOCITIES IN KNOTS)

EOA-334

Fig. 7. U,V, W Wind Components vs. Time.

RAYTHEON COMPANY
EQUIPMENT DIVISION
RAYTHEON

$$V_{\parallel} = u \cos\theta \sin d + v \sin\theta \sin d + w \cos d$$

where u, v, and w are the x, y, and z components of velocity,

θ is the azimuth angle from the x axis, and

d is the cone half angle from the z axis.

It is easy to show that a least squares fit to a set of data consisting of velocities and azimuths, V_i and θ_i, such that

$$\sum_{i=1}^{N} \left[V_i - V_{\parallel}(\theta_i) \right]^2$$

is a minimum, produces a set of equations expressible in matrix form as:

$$\underline{S} = \underline{M}\,\underline{V}$$

$$\begin{pmatrix} \overline{V \cos\theta} \\ \overline{V \sin\theta} \\ \overline{V} \end{pmatrix} = \begin{pmatrix} \overline{\cos^2\theta} & \overline{\sin\theta\cos\theta} & \overline{\cos\theta} \\ \overline{\sin\theta\cos\theta} & \overline{\sin^2\theta} & \overline{\sin\theta} \\ \overline{\cos\theta} & \overline{\sin\theta} & 1 \end{pmatrix} \begin{pmatrix} u \sin d \\ v \sin d \\ w \cos d \end{pmatrix}$$

where the bar over a quantity denotes the average as in this example:

$$\overline{V \cos\theta} = \frac{1}{N} \sum_{i=1}^{N} V_i \cos\theta_i$$

The problem of calculating u, v, and w from the V_i and θ_i is thus reduced to the simple task of inverting the matrix $\underline{M}$:

$$\underline{V} = \underline{M}^{-1}\,\underline{S}$$

If the points are uniformly spaced over π or 2π radians, the matrix becomes

$$\underline{M} = \begin{pmatrix} .5 & 0 & 0 \\ 0 & .5 & 0 \\ 0 & 0 & 1 \end{pmatrix}$$

and the data processing involves only calculation of the matrix $\underline{V}$ and a few simple mathematical operations.

A sample of the data for a typical VAD scan is shown in Figure 6. The quantized curve is the raw data with its sign reconstituted by estimating the wind direction using the highest velocity and associated angle with the assumption of zero vertical wind. The smooth curve shows a least square fit to a sine wave which was performed in real-time, using a simple algorithm. Figure 7 shows a set of u, v, and w components as functions of time from data collected with a VAD scan. It is obvious in Figure 6 that some errors occurred in the sign reconstitution process. These may be eliminated by an iterative process which uses the calculated u, v, and w to determine corrected zero crossings followed by a new least squares fit. The process will reach a final value usually within two or three iterations and will seldom change u, v, or w by more than 2%.

It should be noted at this point that the data includes 360 data points, from which 360 independent parameters may be obtained. This may be considered in the following way.[5] If the wind field in the plane of the scan can be expressed as a

power series

$$\bar{V}(x,y) = \bar{V}(o,o) + \sum_{n=1}^{\infty} \bar{a}_{xn} x^n \sum_{m=1}^{\infty} \bar{a}_{yn} y^n$$

where the origin of coordinates is at the scan center and a_{xn} and a_{yn} are unknown constants, then the Fourier series of $V(\theta)$ gives information about $\bar{V}(o,o)$ from the zeroth and first terms, and about a_{xn} and a_{yn} from the nth term. Calculation of $\bar{V}(o,o) = u\hat{x} + u\hat{y} + w\hat{z}$ is the same as in the above least square fit algorithm.

This has two interesting results: first, it states that it is possible to obtain some information on the wind velocity field inside the circle, and second, it states that it is not necessary to make the assumption of a uniform wind field over the scan in order to obtain a good estimate of the velocity vector at the scan center. Thus, the system actually measures an average velocity over a region smaller than the circle.

4. DESCRIPTION OF THE SYSTEM

The coherent CO_2 LDV is a laser system capable of measuring line-of-sight atmospheric velocity using the Doppler shift as described in the previous section. The optical components transmit the laser radiation, receive it, and recombine it with the reference beam to generate the frequency shift. The LDV processor measures this frequency shift, digitizes and

inputs the data, including the spatial coordinates of the point at which the velocity was measured, to a mini computer. Through the use of the mini computer, the system is capable of operation at a remote site with a quick look capablity for system performance and data quality evaluation. The mini computer performs real time processing to prepare the data for output to a large computer for the final processing. A block diagram of this system is shown in Figure 8 where each of the blocks are described below:

The laser is a Raytheon model LS-10A with a nominal output power of 17 watts. The output beam is TEM_{oo} with the $1/e^2$ intensity points at a diameter of about 7 mm. The horizontal polarization is determined by Zinc Selenide (ZnSe) Brewster windows on the ends of the discharge tube.

In the interferometer, the reference beam is obtained from the transmitter and combined with the reflected radiation. The telescope is an f/8 Cassegrainian with a one foot primary. It serves the purpose of expanding the beam and controlling the range to focus by means of a moving secondary. The detector is a liquid nitrogen cooled (77K) Lead Tin Telluride chip of about 250 μm width. It is mounted in a dewar capable of holding liquid nitrogen for 8 hours. The reference beam power of a few milliwatts is sufficient to provide shot noise limited operation of the detector over a bandwidth greater than 60 MHz.

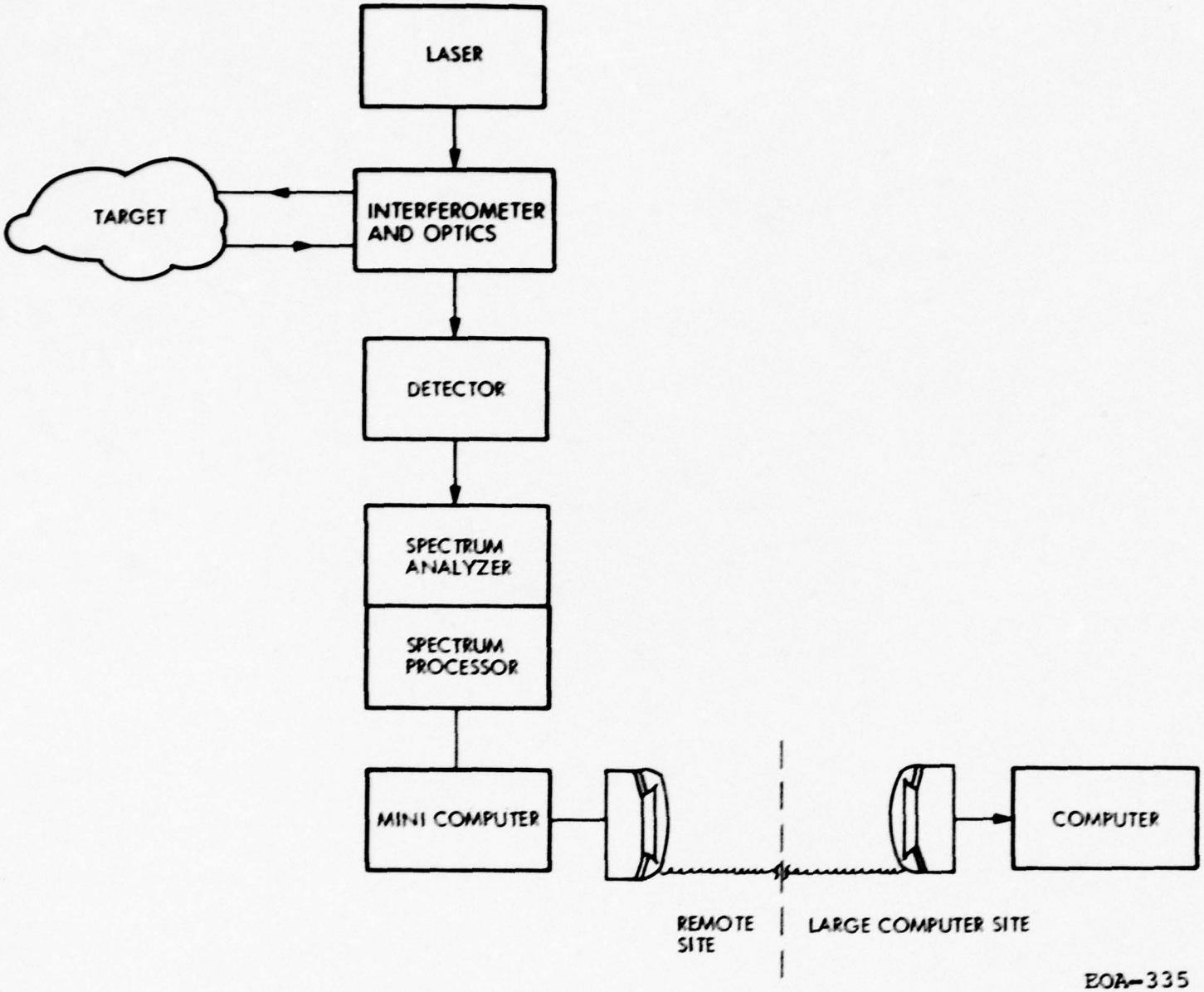

Figure 8. System Block Diagram

The spectrum analyzer and spectrum processor consist of a SAW delay line spectrum analyzer followed by a digital processor which provides for temporal and spectral integration, amplitude, low frequency and frequency width thresholds, linear or logarithmic output ranges and digital output of the selected spectrum and parameters. The SAW delay line is ideally suited for spectral analysis because of its high duty cycle frequency measurements. The processor bandwidth is 10 MHz with a resolution of 100 kHz. The amplitude has 256 discrete levels.

Parameters which are available to the computer are:

I_{pk}, the highest amplitude in the thresholded spectrum,

V_{ms}, the frequency (velocity) associated with I_{pk},

V_{pk}, the highest velocity in the threshold spectrum, and

N, the number of velocity filters above threshold.

These are illustrated in Figure 9.

The mini computer is a Raytheon 706 with a cycle time of 1 μsec and 16K of core memory. It is equipped with paper tape facilities, a Tektronix 4010-1 display, a hard copy unit, a time code generator, and an interface to collect data from the system.

For final-processing, the CDC-6700 computer installation

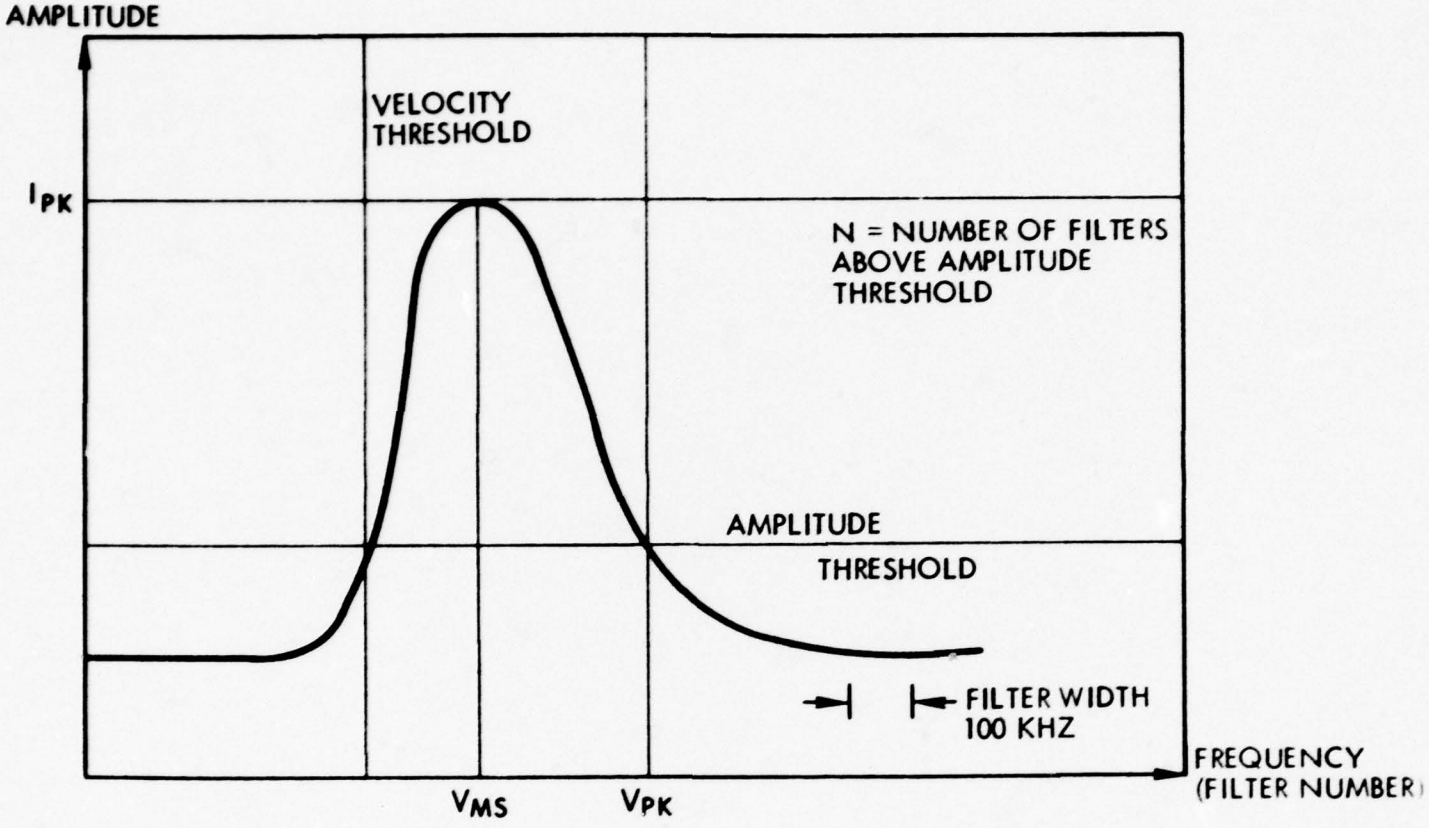

Figure 9. Spectral Parameters

located at Raytheon in Bedford, Mass. is used. This is accessed via phone lines to perform more sophisticated data processing with Fortran programs and plotting routines for display of the processed data.

The scanner consists of a tilted mirror rotating about a vertical axis. The beam enters from above using a bending mirror, and then is reflected from the scan mirror at a 30^{o} angle to the vertical. As the scanner rotates, the focussed spot describes a circle in a horizontal plane above, and centered on, the system.

Figure 10 shows a view of the van in which the system is mounted.

5. PROCESSING

The data obtained from the coherent CO_2 LDV is processed using a real-time correlation routine on a Raytheon 706 mini computer followed by an FFT performed on a CDC-6700. The FFT routine includes numerous displays for evaluation of the data.

An overall flow of the processing is shown in Figure 11 in two parts. The top part is the processing carried out by the Raytheon 706 mini computer installed with the system. The lower part is the processing accomplished by the CDC-6700 at the Raytheon installation in Bedford, Mass.

Use of the two computers permits maximum flexibility in the final processing algorithms while retaining a quick-look

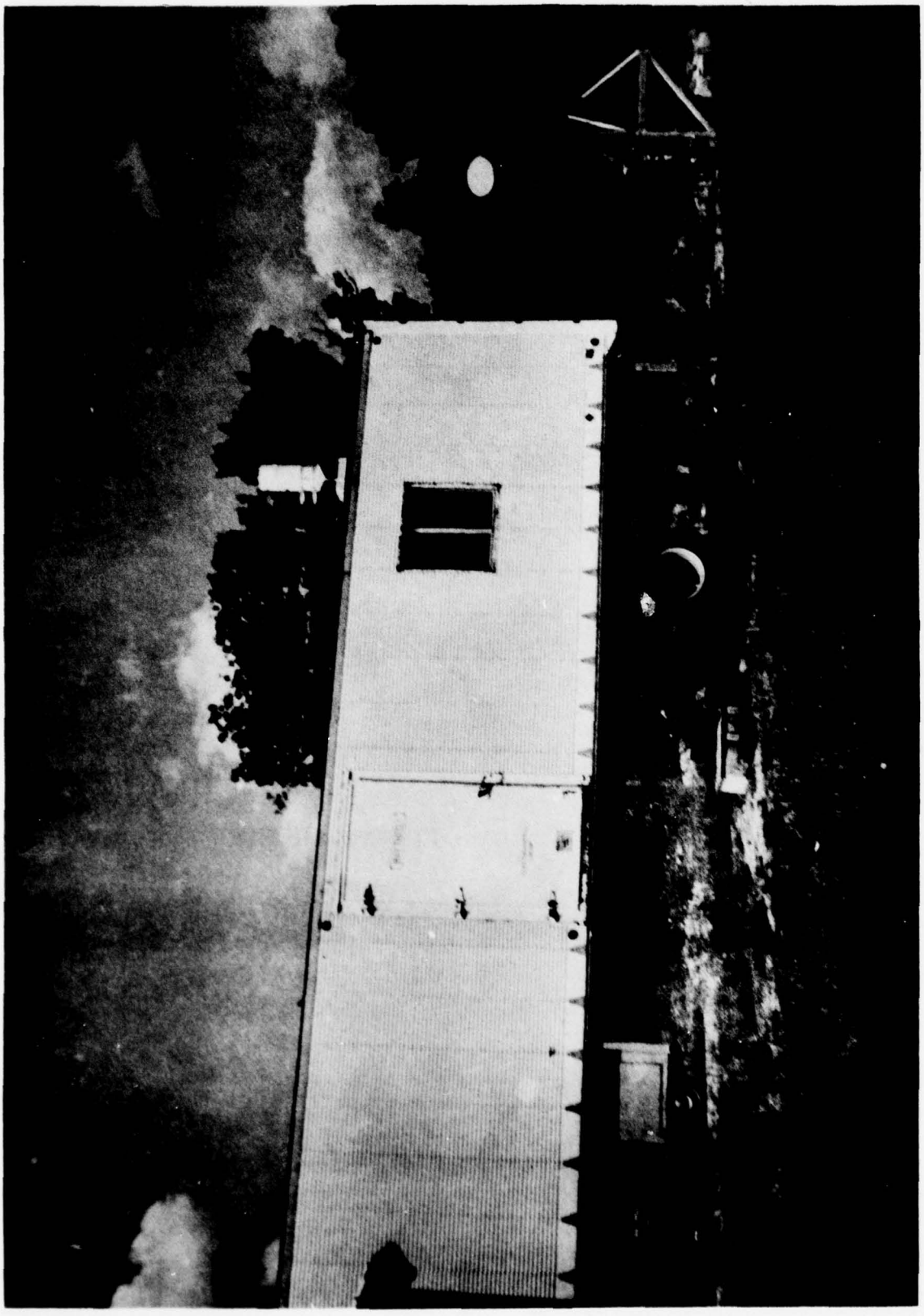

EO-315

Figure 10. Laser System Van

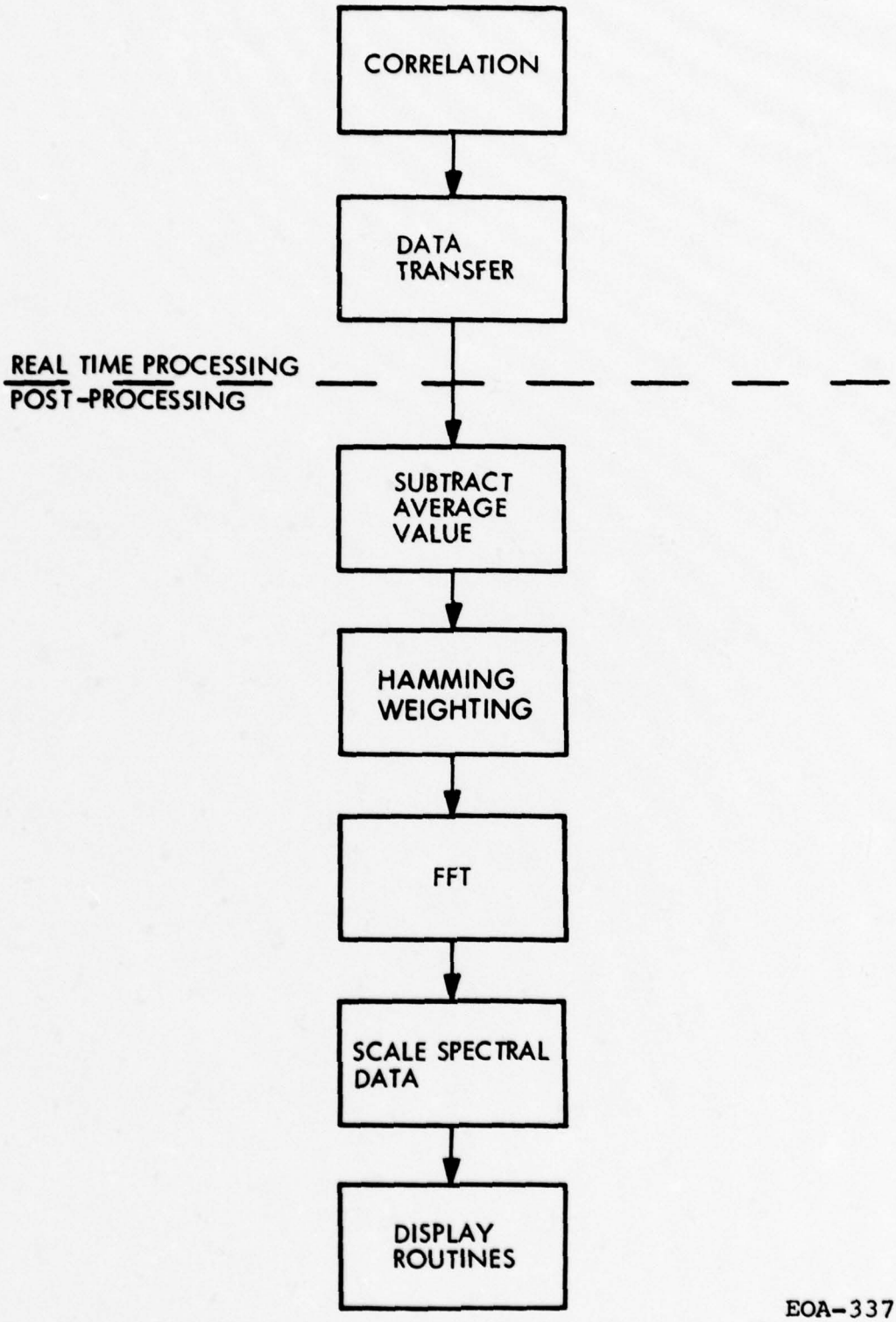

Figure 11. Flow Diagram of Data Processing

capability in the real time data processing phase. The two processing operations are linked by one of two data transfer techniques: by physically carrying the paper tape containing the correlation functions to a terminal that could read it into the CDC-6700, or by feeding the information directly to the 6700 through a telephone link connected to the 706. The following paragraphs discuss separately the processing algorithms used by the two computers.

The velocity information $V(\theta)$ received from a conical scan in the presence of a uniform horizontal wind field would be sinusoidal with a peak occurring when the azimuth of the beam is upwind, a trough when it is downwind and zeros when it is perpendicular to the wind field. The presence of a vertical wind causes a constant offset of this sine wave. The present LDV, as discussed earlier, cannot detect the sign of the line-of-sight velocity and this ambiguity results in a rectification of the sinusoid. A velocity vs. azimuth graph for a uniform wind field with an updraft present is shown in Figure 12, as it would be seen by the LDV after completing one 360° scan around the cone. The information to be obtained is the magnitude of the local velocity averaged over a scan. The technique for obtaining this velocity was outlined in the principles of operation. It is implemented in the following way (see Figure 13). First 360 points are collected and the largest value is found. It is then assumed that any points outside of

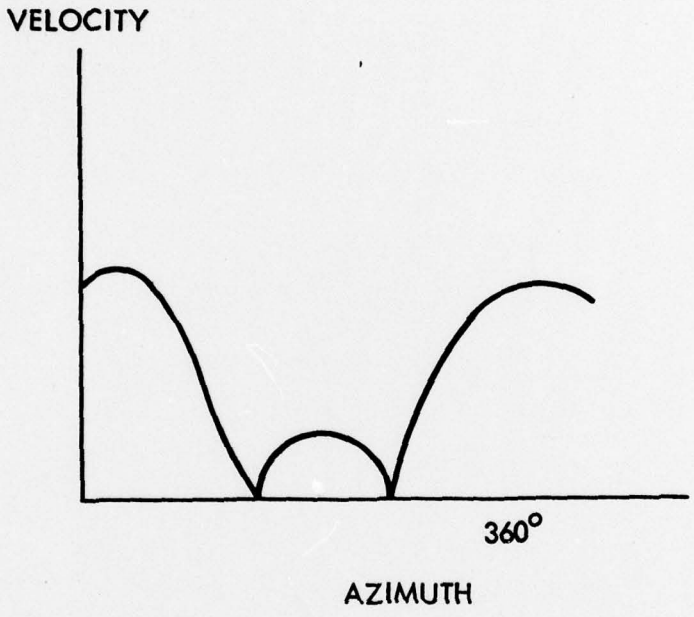

Figure 12. Idealized Raw Data

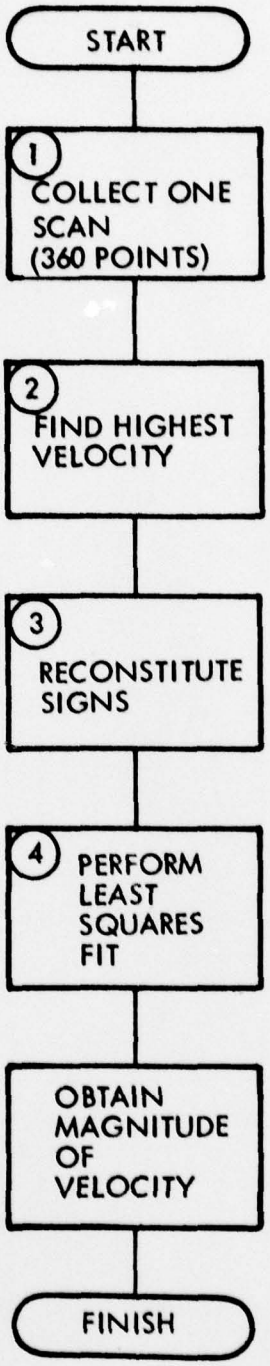

EOA-339

Figure 13. Velocity Calculation

180^{o} bin centered on the largest value were originally of opposite sign. In the reconstruction step all of these rectified points are made negative. The data is now in the form of a rough sinusoid which is least square fitted to the function:

$$V_{\|} (\theta_i) = u \cos\theta \sin\delta + v \sin\theta \sin\delta + w \cos\delta$$

Next, the magnitude of the velocity is calculated;

$$|V| = \sqrt{u^2 + v^2 + w^2}$$

Then, the power spectral density is calculated. This could be accomplished by squaring the magnitude of the Fourier transform of the velocity data, but that would require that every data point be saved so that the transform could be taken at the end of the run. During a typical run, this would amount to many thousands of points. A method employing more economical usage of computer memory is to take Fourier transform of the autocorrelation of the velocity data as described earlier. A 1024 point autocorrelation is employed.

The correlation function Γ_J is computed by the equation:

$$\Gamma(J) = \frac{1}{N_{max}} \sum_{N=1}^{N_{max}} |V_N| \; |V_{N-J}|$$

where J is an index from 1 to 1024

N_{max} is the total number of data points

The process, shown in Figure 14, is as follows: a 1024 word array is filled up with the first 1024 velocities, $|V_1|$ through

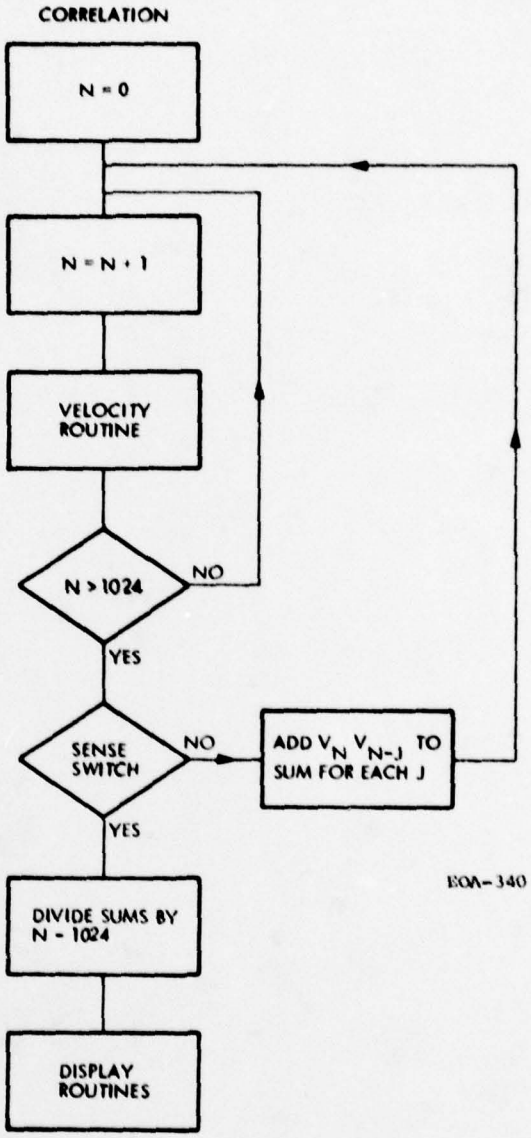

Figure 14. Correlation Process

$|V_{1024}|$, and for each additional data point the appropriate products are added to the sums in the above equation. The run is terminated by the system operator toggling a switch on the 706 computer when enough data has been taken. The correlation function is then output from the computer to the hard copy unit and the large computer.

The final data processing is performed on Raytheon's CDC-6700 computer to determine the energy density spectrum. The first function of the processing program is to check the data format to determine if any errors occurred during the data transmission or paper tape reading process. An opportunity is provided for correcting errors at this point. Next, the program subtracts the average value of the correlation function to remove the large DC contribution to the transform. At this point the data consists of 1,024 values of the correlation function correctly sequenced in time, with the spacing between data points corresponding to the time required for one scan. These values are plotted. The next function of the processing program is Hamming weighting. Whenever a finite data sample is collected, the Fourier transform is equal to the Fourier transform of the desired function convolved with the Fourier transform of a function which is unity for the sample interval and zero elsewhere. The side lobes of this function contribute to a noise floor in the spectrum. This effect is reduced by multiplying the data by a function which has a Fourier transform

with a broader peak, but much lower side lobes. The function used in the present case is the following:

$$\cos^2 \left(\frac{(\pi/2)N}{1024} \right) + .08$$

This function results in a signal-to-noise ratio of approximately 30 dB in the spectrum. After the Hamming weighting is performed, a plot of the data is again produced to show the effects of the weighting. The correlation function is known to be symmetric about T = 0, and this results in the equivalent of a 2048 point transform. The Fourier transform is accomplished using a simple fast Fourier transform (FFT) algorithm. After the Fourier transform is taken, the data consists of spectral data from zero frequency to a frequency corresponding to one-half the inverse of the sample time. Since the correlation function is symmetric, the power spectral density is twice the real part of the Fourier component. These values are printed in tabular form and are also displayed on a logarithmic plot with appropriate scales. The frequency scale is calibrated in units of $(\bar{u}T)^{-1}$ where T is the sample separation. Also shown on this plot is the resolution size based on the size of the circle which is scanned by the system. Displaying the data in a logarithmic format makes it possible to determine the exponent of the spectral density, the amount of energy present in the spectrum, and any deviations from the expected power law. Thus, the final processing algorithm provides the data in a useful format for interpretation as it relates to meteorological

data associated with the experiment.

6. RESULTS

Thirty tests were conducted during the time period from August 1976 through March 1977. Of these, 17 used a simpler velocity processing algorithm where the highest velocity in a scan is used as $|\bar{V}|$, while 13 used the least square fit to a sine wave. These 13 were collected during February and March of 1977. Seven runs in March were correlated with daily meteorological data obtained at Boston, Massachusetts, about 32 km east of the test site. For each of these runs, the wind speed was averaged and a standard deviation obtained to supplement the correlation function and power spectral density plots. The altitude of these measurements was 500 meters. A sample of these plots is shown in Figure 15. The correlation function has it average value removed, and has units of knots^2. The peaks of the power spectral density plot show a -5/3 slope yielding an ϵ of .003 cm^2/sec^3. The weather at the time of the run was clear and warm following a storm the previous day which produced 0.6 inches of rain.

Figure 16 summarizes the results of the data collected during March with the meteorological data. It may be seen that ϵ varies from near 10^{-4} to .04 cm^2 sec^{-3}. High values of ϵ tend to correlate with low barometer readings and precipitation. A phenomenon which is observed on several occasions is a spectrum with two regions of nearly -5/3 slope having different

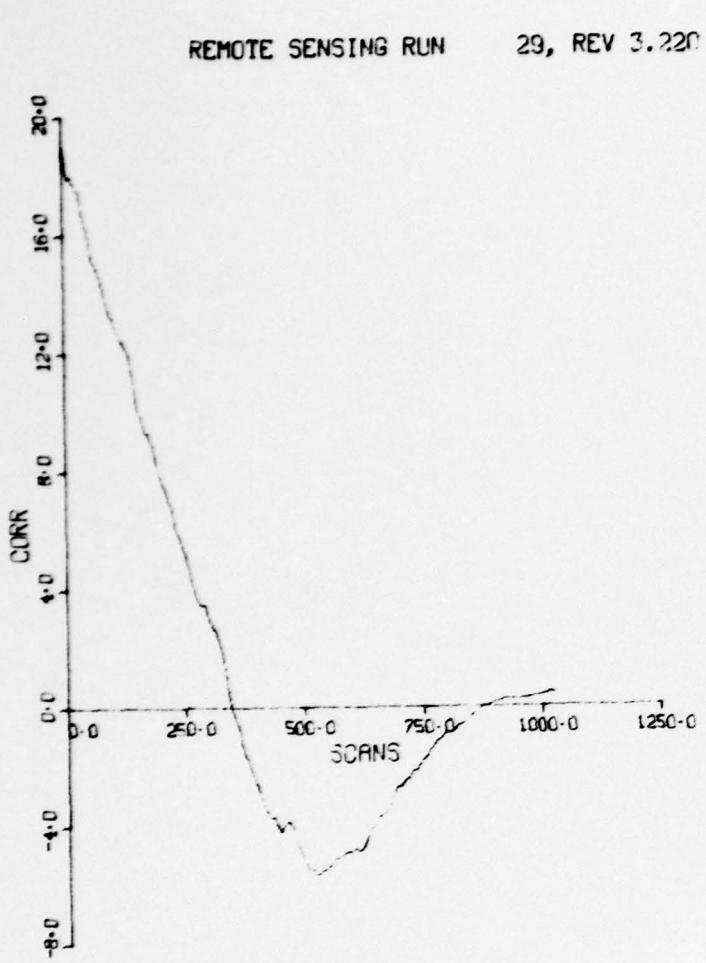

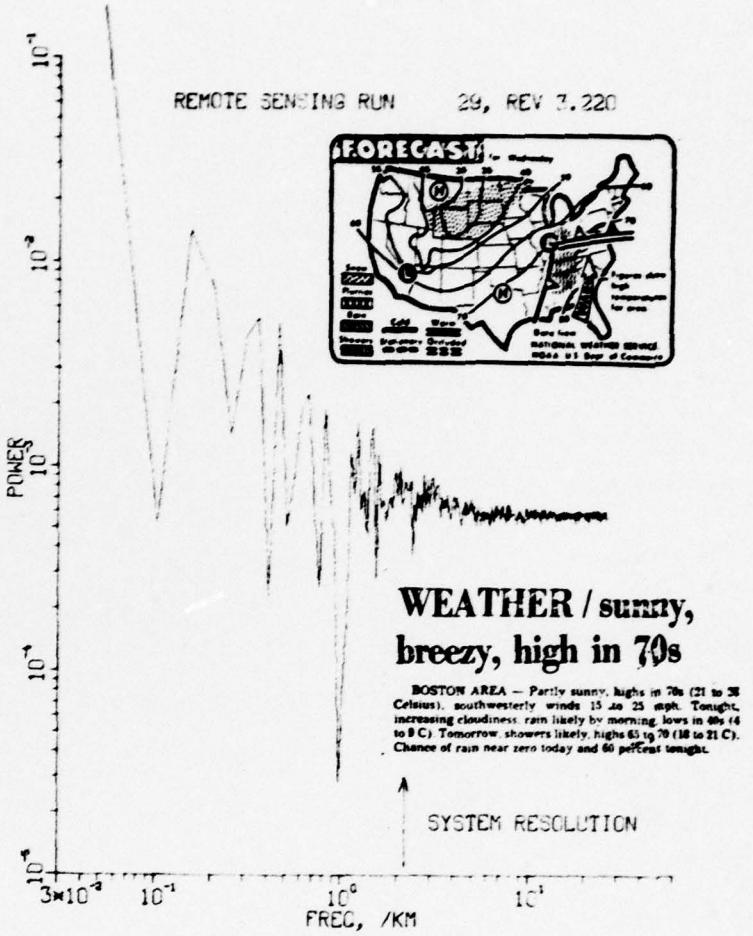

RAYTHEON COMPANY
EQUIPMENT DIVISION
RAYTHEON

EOA-342

Figure 15. Sample Data Output

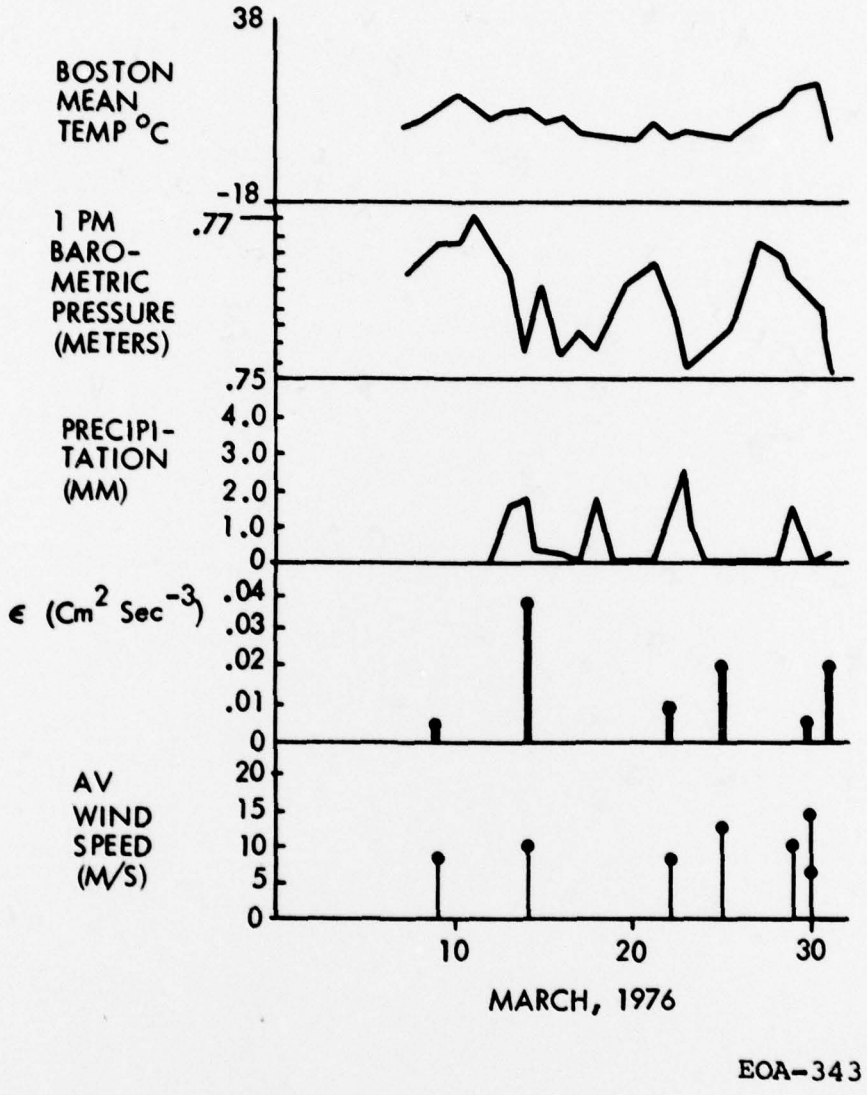

Figure 16. Rass Data Summary.

values of ϵ. This is illustrated in Figure 17 which is from run 27. This run was conducted on 29 March; a cloudy day with showers. A similar phenomenon was observed in run 36 on 31 March under similar conditions as shown in Figure 18.

It is worthwhile to evaluate some of the data collected using the simpler algorithm since it includes two runs during a hurricane. These runs were collected on August 1976 while Hurricane Belle was between Long Island, New York and the Massachusetts-Vermont state line. Unfortunately, the simplicity of the velocity algorithm leads to some erroneous results, including a slope less steep than -5/3. However, the discontinuities described above are clearly visible in Figure 19 with the most structure seen in run 1. After landfall, the hurricane decreased in intensity and the structure in the later run (2) was greatly reduced. For comparison, run 3 was made several days later in clear weather, and shows very little structure.

In summary, several good sets of data have been obtained. The Kolmogorov, -5/3 power law is observed to be met fairly well on most runs. The total turbulent energy increases during storms, and the spectrum often shows multiple regions of -5/3 slope which appear to be correlated with storms. While considerably more data must be collected and analyzed to determine the usefulness of the energy density spectrum in forecasting, the coherent, CO_2 LDV has been demonstrated to be a powerful tool for making meteorological measurements.

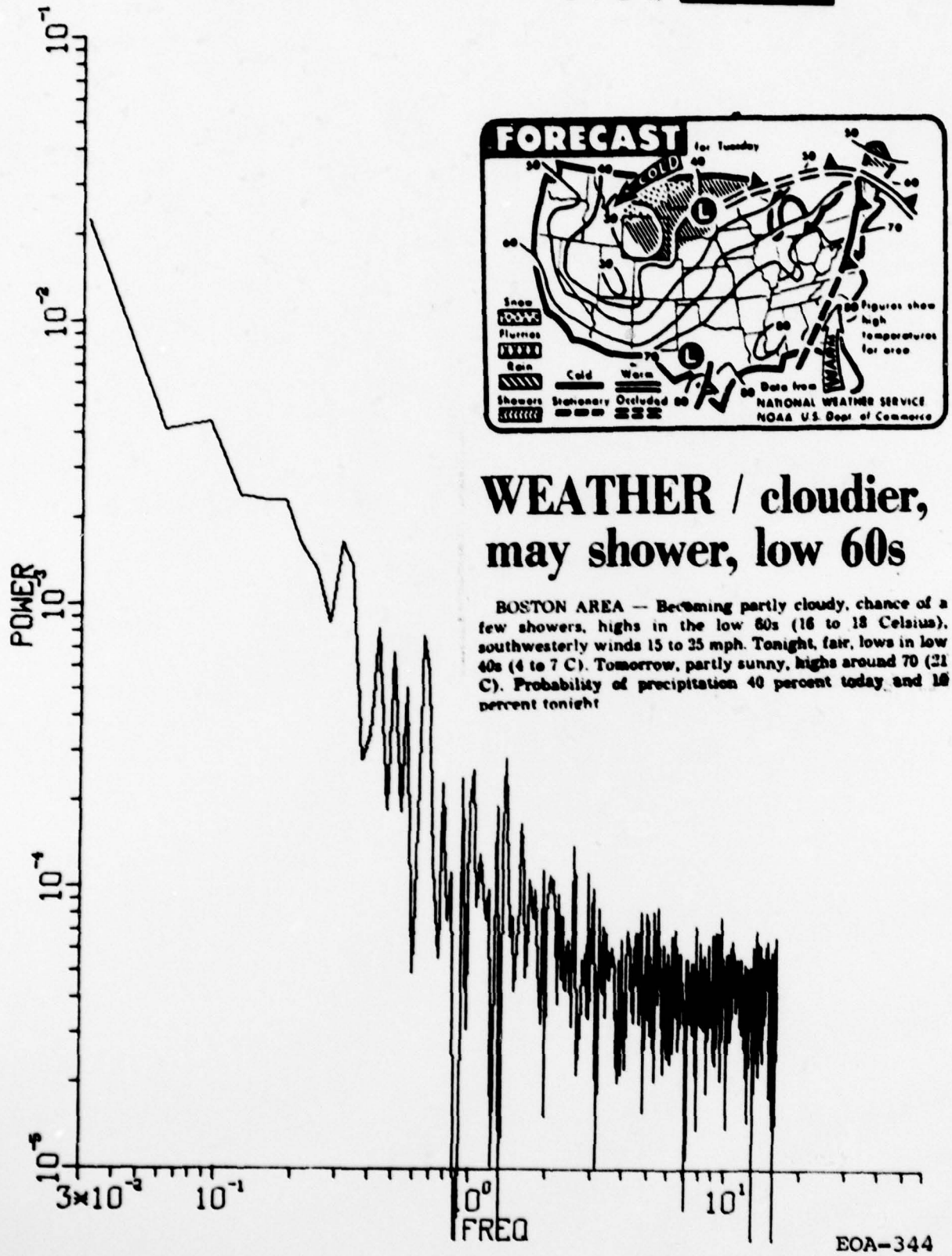

WEATHER / cloudier, may shower, low 60s

BOSTON AREA — Becoming partly cloudy, chance of a few showers, highs in the low 60s (16 to 18 Celsius), southwesterly winds 15 to 25 mph. Tonight, fair, lows in low 40s (4 to 7 C). Tomorrow, partly sunny, highs around 70 (21 C). Probability of precipitation 40 percent today and 10 percent tonight

Figure 17. Typical Power Spectral Density

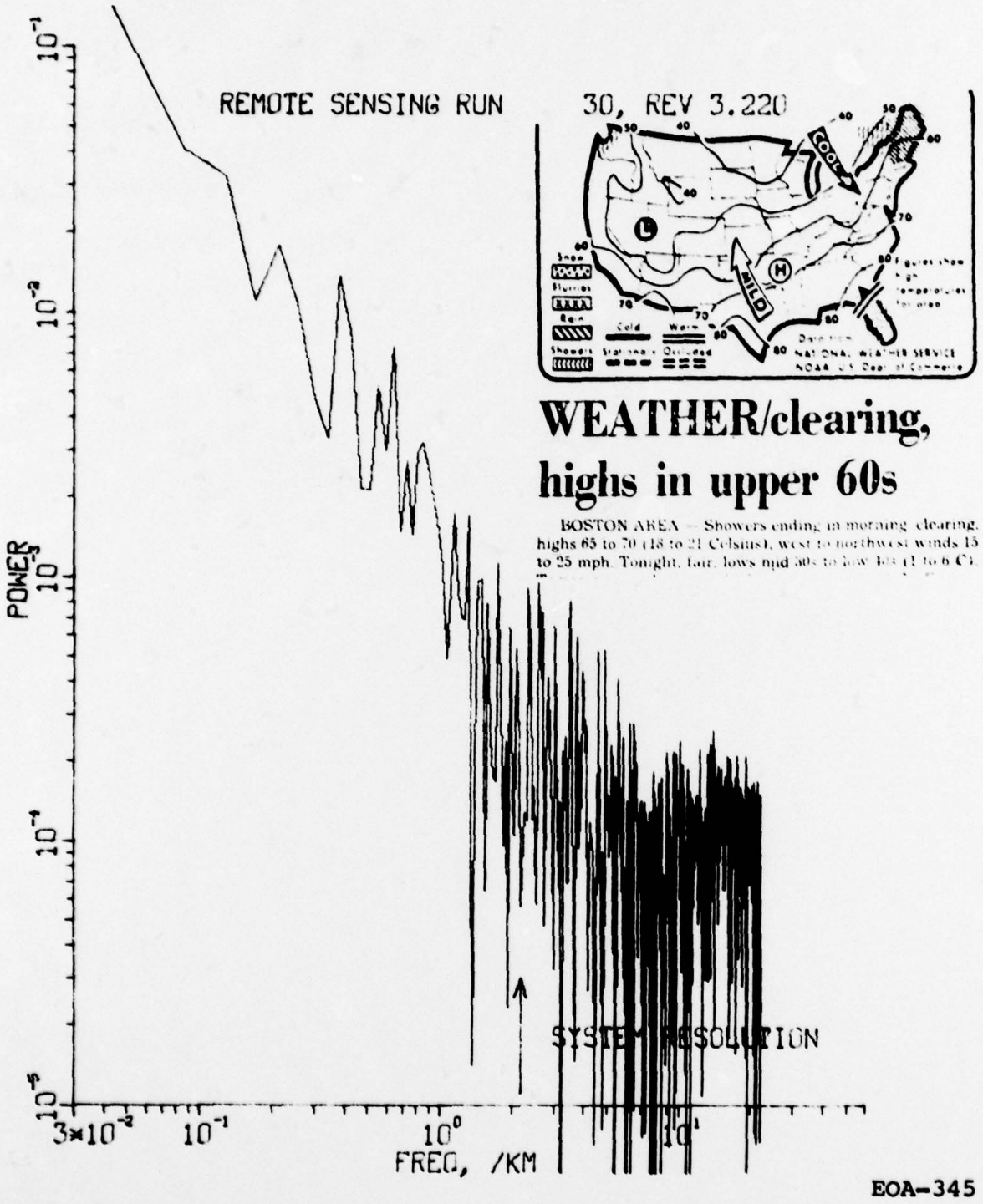

Figure 18. Energy Density Spectrum

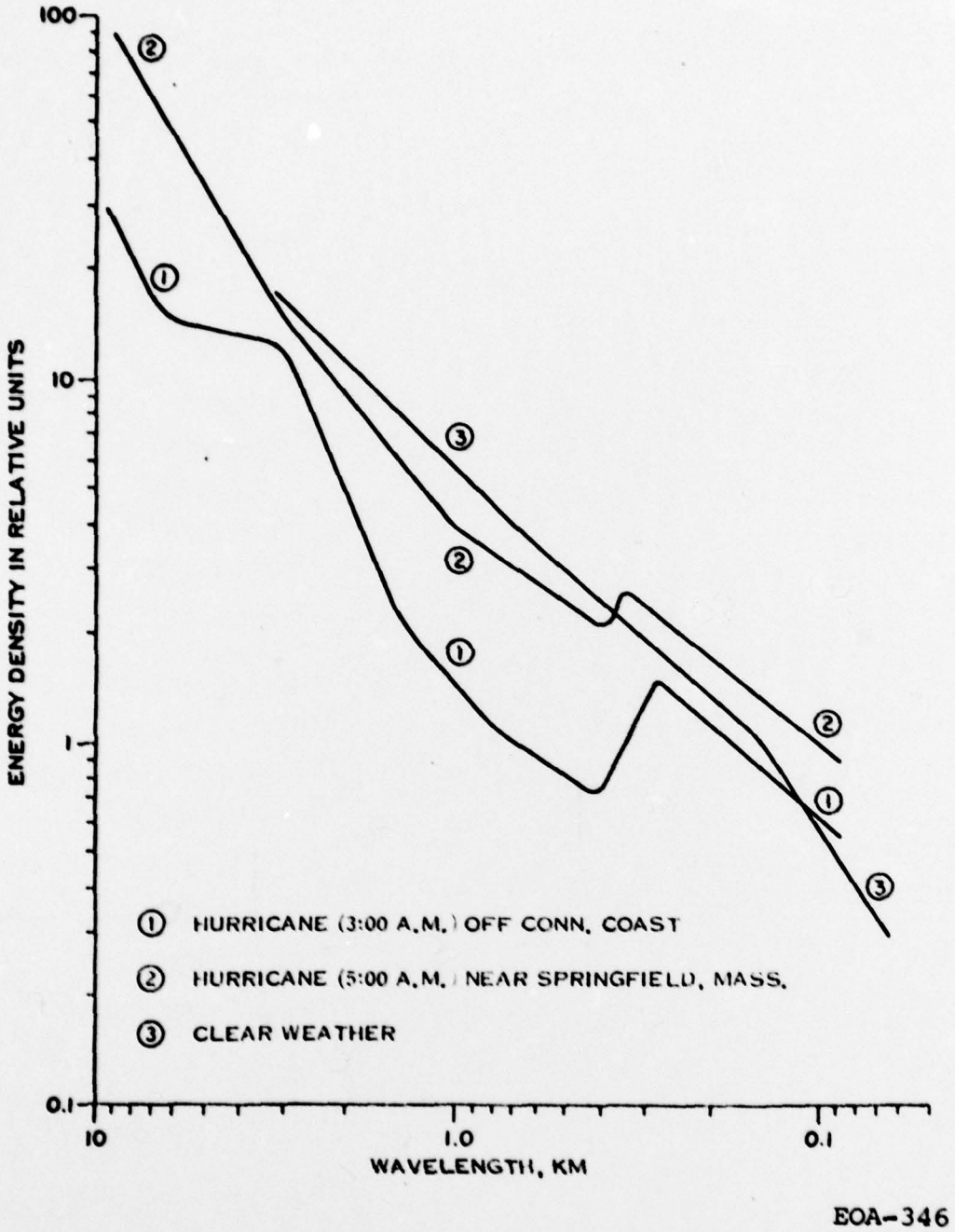

Figure 19. Power Density Spectra of Hurricane Bell

REFERENCES

1. A. N. Kolmogorov, "The local structure of turbulence in incompressible viscous fluid for very large Reynolds' numbers", Doklady Akad. Nauk SSSR, 30, 301 (1941). German translation in "Sammelband zur Statistischen Theorie der Turbulenz", Akademie-Verlag, Berlin (1958), p. 71.

2. A. N. Kolmogorov, "Dissipation of energy in locally isotropic turbulence", Doklady Akad. Nauk SSSR, 32, 16 (1941). German translation in "Sammelband zur Statistischen Theorie der Turbulenz", Akademie-Verlag, Berlin (1958), p. 77.

3. V. I. Tatarski, "Wave Propagation in a Turbulent Medium", translated from the Russian by R. A. Silverman, McGraw-Hill, New York (1961), p. 37.

4. G. I. Taylor, "The Spectrum of Turbulence", Proc. Roy. Society A, Vol. 165, p. 476, 1938.

5. K. A. Browning and R. Wexler, "The Determination of Kinematic Properties of a Wind Field Using Doppler Radar", Journal of Applied Meteorology, 7, 1, (1968)p. 105 - 113.